Cement and Concrete Research xxx (2018) xxx-xxx

Contents lists available at ScienceDirect

Cement and Concrete Research

journal homepage: www.elsevier.com

# Mechanical properties and durability performance of concretes with Limestone Calcined Clay Cement ($LC^3$)

Yuvaraj Dhandapani, T. Sakthivel, Manu Santhanam*, Ravindra Gettu, Radhakrishna G. Pillai

*Department of Civil Engineering, Indian Institute of Technology Madras, India*

ARTICLE INFO

*Keywords:*
Limestone
Calcined clay
Composite cement
Durability
Microstructure

ABSTRACT

The adoption of any binder system for structural concrete depends on the performance characteristics desired for addressing the long-term deformation and durability concerns. The major properties influencing the performance includes the shrinkage characteristics governing the long-term deformation, and durability characteristics related to various transport mechanisms, governing the performance in different service conditions. This paper describes the potential of Limestone Calcined Clay Cement ($LC^3$) for use in structural concrete in comparison with Ordinary Portland Cement (OPC) and fly ash based blended cement (FA30). Three types of concrete mixtures were designed for the study, two based on achieving an equivalent strength grade (M30 and M50 concrete grade) with each binder, and the third with equal binder content and w/b ratio. Mechanical properties such as compressive strength and elastic modulus, and autogenous and drying shrinkage, along with various durability parameters of the different concretes were assessed. Oxygen permeability, rapid chloride penetration, chloride migration, resistivity development and water sorptivity were the various parameters considered for evaluation of durability performance. The results indicate the superiority of $LC^3$ binder over other binders in producing durable concrete, especially in a chloride laden environment. The major reason for the better performance was attributed to the more compact and dense microstructure of the system with the $LC^3$ binder against OPC and FA30. The drying shrinkage performance was seen to be similar for concrete with all three binders.

## 1. Introduction

Research on alternative binders, to reduce the impact of cement production on natural resources and associated carbon footprint in the production process [1–3], has been ongoing for a long time. Mineral admixtures, often known as Supplementary Cementitious Materials (SCMs), are mainly industrial waste/residues (mainly fly ash and slag) that have a potential to reduce the clinker content in the cement. The primary issue with high replacement levels of these materials (especially fly ash) has often been the adverse effects on early age properties like delayed setting and strength development in the concrete [4]. In addition, the use of these materials is limited by the accessibility of the specific industry (i.e., thermal power plant or steel manufacturing unit) to the cement production plants. To meet the demands of sustainable production and application of cement, it is necessary to develop new cementitious materials that can produce a good mechanical performance at early ages, similar to Ordinary Portland Cement (OPC), and remain durable in different service conditions. Limestone Calcined Clay Cement ($LC^3$) has shown promise in this regard [5,6]. $LC^3$ is a ternary binder system consisting of calcined clay and limestone used in conjunction to make a composite cement [7].

Studies on cement mortars by Antoni et al. [8] showed that replacement of cement with a blend of calcined clay and limestone produced a comparable mechanical performance as plain Portland cement. The wide availability of calcined clay can cater to the needs of increasing demand for cement substitution materials. Kaolinite clay produces a reactive amorphous phase when heated at 600–800 °C [9]. In the presence of limestone, the reactive part of calcined clay forms an increased amount of AFm phases (monocarboaluminate and hemi-carboaluminate) leading to a complementary reactivity between calcined clay and limestone [8,10]. The amount of limestone reacted is dependent on the amount and nature of the aluminate sources [11]. The kaolinitic content of the calcined clay is the most prominent factor governing the mechanical performance of calcined clay based binder systems [12]. Calcined clay being a highly reactive pozzolan also improves mi-

* Corresponding author.
*Email address:* manusanthanam@gmail.com (M. Santhanam)

https://doi.org/10.1016/j.cemconres.2018.02.005
Received 31 July 2017; Received in revised form 15 November 2017; Accepted 6 February 2018
Available online xxx
0008-8846/ 

crostructure development and refines pore structure at an early age [13].

The addition of limestone tends to have varied effects on performance of blended cements. A detailed report summarizing the fresh and hardened concrete properties with limestone additions (up to 15%) in the cement is available [14,15]. The results of this report are acknowledged in ASTM C595 [16]. Further, studies on concrete performance by Githachuri and Alexander [17] on PLC (Portland limestone cement, containing 20% limestone) show similar or marginally lower durability parameters compared to concrete made with PC. In addition, the use of fly ash and slag as a blending material with PLC was found to bridge the effect of dilution caused due to replacement of Portland cement with limestone. The use of higher amount of limestone content (>20%) necessitates lowering of water-cement ratio to produce concretes with similar durability performance [18].

A review on the use of metakaolin and calcined clay as pozzolan for concrete by Sabir et al. [19] outlined several positive effects of metakaolin addition on the pore structure and concrete properties. Substituting a part of Portland cement upto 25% metakaolin improved resistance to chloride with a lower diffusion coefficient and an increase in diffusion reduction factor being registered with increasing level of substitution [20]. Khatib and Clay studied the absorption characteristics of concrete with increasing substitution of metakaolin and confirmed a reduction in the water absorption in the system because of lowering of porosity in the concrete [21].

Taking advantage of the distinct contribution of the limestone and SCM as binder components, studies with a combination of limestone and common SCM (metakaolin, slag and fly ash) have often been attempted [8,22–26]. In [8,23], the positive impact on hydration and strength development characteristics of metakaolin-limestone composite binder is discussed. In [22,25] [24,26], the use of slag-limestone combination on mortar strength development, hydrated phases, and pore sizes were explored in detail. In the case of fly ash-limestone combination, the use of a minimal 5% limestone along with fly ash (30%) showed an improvement in the strength development characteristics compared to binary blended cement with only fly ash (35% replacement) [27]. Further, in a study evaluating the quality of calcined clay for cement replacement [12], the effectiveness of lower grade kaolinite clay (>40% kaolinitic content) was explained. The relevance and applicability of such lower grade calcined clay on concrete properties with $LC^3$ needs to be further explored for concrete usage.

Detailed studies on the effect of composite binders on the performance of concrete systems are limited. The sustainable application of any new cementitious system depends mainly on the performance of concrete. A wide range of concrete applications for both structural and non-structural purposes in different service environments implies that concrete properties should meet several different requirements such as compressive strength evolution, elastic modulus, volume change effects (shrinkage and creep), and durability properties such as resistance to ionic ingress, gas ingress, and moisture ingress. The rise in the demand for cementing materials necessitates the replacement of increasing amounts of clinker with the substitute materials to reduce the ecological impact of clinker production. Sustainability involves both optimal design of binder mixture as well as obtaining an improvement in the performance of the binder. It is necessary that both these intrinsic requirements of any new binder system are evaluated, for these new binders to perform as a mainstream industrial cement. This study reports a detailed investigation on the mechanical and durability properties of concretes made with $LC^3$ as an alternative binder system in comparison to widely adopted OPC and fly ash based PPC cementitious systems. Specifically, this paper presents:

i. Compressive strength evolution in concrete designed for two different strengths categories with each binder, and one concrete mix with equivalent binder content and water-binder ratio.
ii. Investigation on the shrinkage development (autogenous and total shrinkage) in concrete made with different binder systems after 28 days of initial curing.
iii. The performance of the concrete with respect to transport properties such as chloride ingress, moisture ingress and gas penetrability. The suitability of concrete made with the different binder systems is also assessed for adoption in a particular service environment based on performance based criteria.
iv. The variation in porosity and pore structure parameters and a study on the microstructure of hydrated paste, to give an insight into the microstructural variation and consequential effect on the performance of the $LC^3$ binder system is also discussed.

## 2. Experimental procedure

### 2.1. Materials

Ordinary Portland Cement (53 grade) conforming to IS 12269 [28] was used. Siliceous fly ash from Ennore near Chennai was used to produce a lab scale Portland Pozzolana Cement or PPC (named as FA30, with 30% substitution level; 70% OPC + 30% fly ash). $LC^3$ from a trial industrial production carried out in Gujarat, India was used. The composition of clinker: calcined clay: limestone: gypsum is 50:31:15:4 for the $LC^3$ blend used in this study. It is noteworthy to mention that the clinker used in $LC^3$ is different compared to the OPC. The chemical composition of the clinker used in $LC^3$ is also mentioned in Table 1. Arun et al. [5] have elaborated the cement properties from this industrial production of the $LC^3$. The gypsum in this system was optimized to ensure that the reaction of the aluminates (from calcined clay) are pushed beyond the major calcium silicate reaction as seen in isothermal calorimetry. The chemical composition of the materials used in the

**Table 1**
Chemical composition of materials used in the study.

| Oxides | OPC | Class F fly ash | $LC^3$ | | |
|---|---|---|---|---|---|
| | | | Clinker | Calcined clay | Limestone |
| CaO | 64.59 | 1.28 | 63.81 | 0.09 | 48.54 |
| $SiO_2$ | 19.01 | 59.32 | 21.12 | 58.43 | 10.07 |
| $Al_2O_3$ | 4.17 | 29.95 | 5.24 | 24.95 | 1.74 |
| $Fe_2O_3$ | 3.89 | 4.32 | 3.41 | 5.08 | 1.62 |
| MgO | 0.88 | 0.61 | 3.06 | 0.19 | 0.467 |
| $Mn_2O_3$ | – | – | 0.06 | – | 0.035 |
| $Na_2O$ | 0.16 | 0.16 | 0.32 | 0.05 | – |
| $K_2O$ | 0.59 | 1.44 | 0.19 | 0.21 | 0.13 |
| $TiO_2$ | 0.23 | – | 0.10 | 1.41 | 0.206 |
| $SO_3$ | 1.70 | 0.16 | 0.63 | – | 0.01 |
| LOI | 1.40 | – | 0.98 | 9.58 | 37.09 |

study is presented in Table 1. The particle size distribution by laser diffraction, obtained after dispersing the powder in Isopropanol is given in Fig. 1. It is seen that the fly ash used in this study contained a larger amount of coarser particles than plain Portland cement. In the case of $LC^3$, there were more finer particles due to the limestone powder and calcined clay. The physical properties of the blends and cement mortar compressive strength at w/b ratio of 0.42 are also presented in Table 2. The fine aggregate used for the concrete was graded river sand with 4.75 mm nominal maximum aggregate size, and a mixture of 10 mm and 20 mm crushed granite was used as coarse aggregate. Polycarboxylic ether (PCE) based superplasticizer (SP) with a solid content of 34% was used to achieve the target slump of 80–120 mm.

### 2.2. Mixture proportioning

The concrete mixes were optimized from a large set of trial mixes. Three binder contents (310 kg/m$^3$, 340 kg/m$^3$ and 360 kg/m$^3$) and range of water-binder ratios between 0.4 and 0.6 were adopted to prepare concretes for compressive strength evaluation. The mix design was carried out on a volumetric basis, in which the binder content and water-binder ratio was fixed, and the remaining volume was proportioned between fine aggregate and coarse aggregate, in the approximate ratio of 40:60 respectively. Further, the coarse aggregate consisted of the 10-mm aggregate and 20-mm aggregate in the ratio of 40:60 respectively. The superplasticizer (SP) addition was also optimized to achieve a target slump of 80–120 mm in the trial mixes. From the study of trial mixes, the final concrete mixes with two equivalent 28$^{th}$ day compressive strength were chosen. The details of the nine mixes chosen for further investigation are given in Table 3. The two strength grades include M30 and M50 (indicating a 28-day characteristic compressive strength of 30 and 50 MPa respectively), which are representative of a normal strength concrete and moderate strength concrete used in major applications. In order to achieve the characteristic strength values, a mean strength of 38 MPa (±5 MPa) and 60 (±5 MPa), on a 100-mm cube, was fixed as the acceptable target for M30 and M50 grade of concrete respectively. In the equivalent strength category, the mixes were proportioned to produce similar characteristic strength with the three binders. This equivalent strength approach attempts to demarcate the performance of the different binders in the practical scenario of application for structural concrete (where the designer typically specifies only the compressive strength). Apart from the two equivalent strength grade mixes, an additional concrete mix with the same binder content and water-binder ratio was also chosen as a benchmark to assess the performance of different binder systems.

The concretes were mixed in a pan mixer at 25 rpm in a temperature of 27 ± 3 °C. The fresh properties such as initial slump and fresh unit weight were measured. The specimens were cast and placed in a laboratory condition for a period of 24 h, after which the concrete specimens were moved to a moist room (> 90% RH) until the specified age of testing.

### 2.3. Test methods

#### 2.3.1. Compressive strength and elastic modulus

Concrete cubes of 100 mm size were prepared for assessing the evolution of compressive strength of the different concrete mixtures. Concrete cubes taken from the moist room were tested for compressive strength at 2, 7, 28, 90 and 365 days as per IS 516 [29]. Static modulus of elasticity test on cylindrical specimens of 150 mm diameter and 300 mm height was conducted as per ASTM C469 [30]. Both the tests were performed on a 3000 kN (accuracy of ±1%) compression testing machine. For the elastic modulus, the cylindrical specimens were loaded to 40% of the compression strength for 3 cycles and the slope of the load-displacement response on the third cycle was noted as the elastic modulus.

#### 2.3.2. Autogenous and drying shrinkage

Shrinkage studies of concrete were carried out on 150 mm diameter and 300 mm height cylinders and 75 mm × 75 mm × 285 mm (as per ASTM C 157 [31]) prism specimens. The entire shrinkage test was performed after 28 days ($t_0$) of curing in the moist room. The specimens were then stored at 25 °C and 65% relative humidity inside the laboratory. In the case of autogenous shrinkage, the specimens were wrapped with two layers of aluminum foil tape of thickness 0.06 mm to avoid any loss of moisture from the specimen to the surrounding atmosphere. For the total shrinkage measurement, the ends of the cylinders and prisms were wrapped to avoid three-dimensional strain. The ratio of volume to surface area was 37.5 and 18.75 for cylinder and prismatic specimens respectively. For measuring the strain on cylindrical specimens, demountable mechanical (DEMEC) strain gauges were fixed using epoxy adhesive on the surface in the longitudinal direction. A gauge length of 150 mm was adopted, and measurements were taken at two points on circumferentially opposite sides. Similarly, the prisms were tested for change in length using an extensometer with an accuracy of 0.001 mm. The mass of the specimens was also recorded during each measurement (balance with an accuracy of 0.001 kg). The results are reported as an average of 3 specimens, and shrinkage strains up to 400 days are reported in each case.

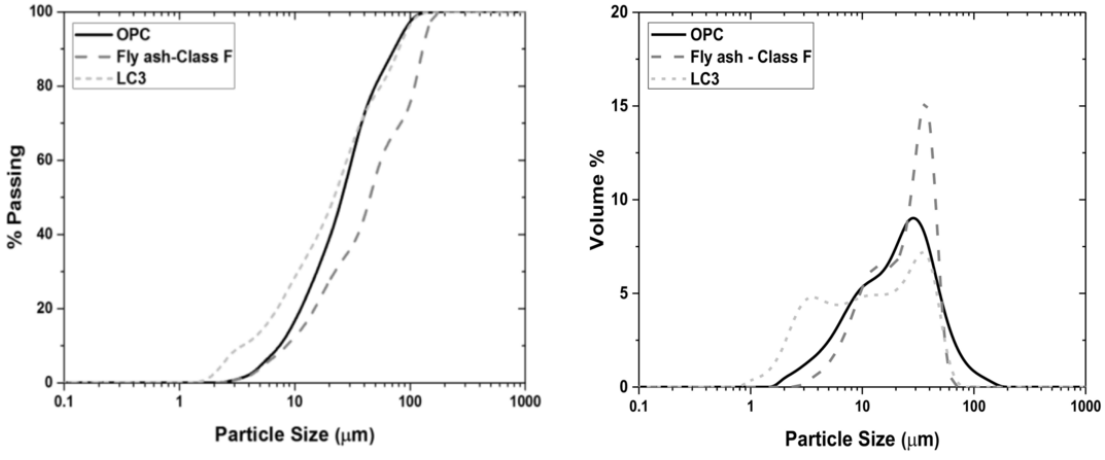


**Fig. 1.** Particle size distribution of the materials. a) Percentage passing and b) volume distribution of particles in different sizes.

**Table 2**
Physical characteristics of OPC, FA30, and $LC^3$ cement.

| Physical characteristics | OPC | FA30 | $LC^3$ |
|---|---|---|---|
| Specific gravity | 3.16 | 2.77 | 3.01 |
| Consistency (%) | 30 | 31 | 33 |
| Initial setting time (min) | 124 | 120 | 101 |
| Final setting time (min) | 245 | 280 | 165 |
| Blaine's fineness ($m^2$/kg) | 340 | 330 | 520 |
| Soundness (mm) | 0.2 | 0.2 | 0.1 |
| Mortar compressive strength at 28 days (MPa) | 61.0 | 46.0 | 43.7 |

#### 2.3.3. Resistivity of concrete

The resistivity of concrete was assessed by Wenner 4-probe resistivity meter (Resipod Resistivity meter) on the sides of saturated cylindrical specimens of 100 mm diameter and 200 mm height [32,33]. Three measurements were taken at three different locations on the cylindrical surface of the specimens, and the test was carried out on three specimens. A total of 27 readings were taken and the average is reported. The measurements were taken immediately after moving specimens from the moist room to avoid any effects of specimen drying influencing the resistivity value. All measurements were taken in laboratory conditions of 23 ± 3 °C.

#### 2.3.4. Resistance to chloride ingress

The resistance to chloride ingress was evaluated using two different migration experiments. The rapid chloride penetration test (RCPT) as per ASTM C1202 was adopted to get a qualitative measure of the concrete's resistance to chloride ingress and Accelerated Chloride Migration Test (ACMT) was also adopted to estimate the migration coefficient of the concrete. Six specimens of 50 mm (±2 mm) thickness each were prepared from two 100 mm diameter cylinders for these experiments. The average of three specimens is reported in both cases. The RCPT gives an indication of chloride resistance of concrete in terms of the total charge passed on a saturated concrete specimen [34].

The Accelerated Chloride Migration Test was conducted as per NT build 492 [35]. This gives an estimate of the non-steady state chloride migration coefficient, which serves as a measure of the rate of chloride ingress. Based on the initial current obtained for an applied electrical potential of 30 V, the final voltage and test duration was fixed from the recommendation given in [35].

#### 2.3.5. Gas permeability

The South African oxygen permeability test was adopted to measure the gas permeability coefficient of the concrete. Four specimens of 69 mm diameter and 30 (±2) mm thickness were prepared using cores extracted from 150 mm cubes. The specimens were conditioned as per the guidelines in the South African Durability Index Manual [36]. Permeability was assessed on a falling head permeability cell. The Schematic of the cell and details of the experimental set up are explained in detail elsewhere [36–38]. The negative logarithm of the Darcy's permeability coefficient is represented as Oxygen Permeability Index.

#### 2.3.6. Water sorptivity and porosity of concretes

After the oxygen permeability measurement, the same specimens were tested for capillary water absorption by placing them in a saturated lime solution inside a tray. The liquid level was maintained up to a level of 2 mm from the bottom of the specimen. The mass of the specimens (surface saturated condition on the immersed side; measured to an accuracy of 0.01 g) was recorded at the time intervals suggested in the Durability Index manual. The final measurement of the mass after vacuum saturation was also taken after a day to estimate porosity. The sorptivity index was calculated by normalizing the slope of the plot between capillary mass rise and square root of time to the total water absorption per unit thickness of the specimens [36]. The porosity was computed from the difference in the initial dry weight and final weight after vacuum saturation divided by the volume of the specimen [39]. Four specimens were used for both the measurements.

## 3. Test results and discussions

### 3.1. Mechanical properties

#### 3.1.1. Compressive strength and elastic modulus

The compressive strength of different concrete mixes is presented in Fig. 2. The evolution of compressive strength in M30 and M50 concrete mixes was comparable for the OPC and $LC^3$ concrete mixtures up to 28 days. This is despite the fact that the $LC^3$ M50 had a lower binder content (as seen from Table 3) to produce the similar target strength, which signifies improved strength potential with $LC^3$ binder systems. However, for the FA30 concrete mixes, which had a lower water content in the mix to attain similar $28^{th}$-day strength, the early age strength characteristics were found to be lower as seen in Fig. 2. There was a greater increase in the compressive strength at later ages (from 28 days to 365 days) in the FA30 and $LC^3$ mixes as opposed to the OPC system. In addition, the M30 mixes of FA30 and $LC^3$ showed a marginally higher increase in the compressive strength than M50 concretes. The prolonged pozzolanic reaction contributes to this development [40].

In the case of common mixes (i.e., mixes with same binder content and w/b), the strength of concrete with $LC^3$ binder was found to be higher at all the ages. This exhibit the effect of better hydration characteristics of the $LC^3$ binder system on the mechanical properties of the concrete. The results indicate that with similar mixture proportion, $LC^3$ binder can produce better compressive strength evolution in concretes than OPC and FA30.

The static elastic modulus of the different concrete mixes is shown in Fig. 3(a). The results indicate that the elastic modulus of the concrete was similar for concretes with all the binder systems. This indicates that concrete made with $LC^3$ can have similar mechanical performance characteristics for structural applications as the other conventional binder systems. The correlation between elastic modulus and compressive strength (presented in Fig. 3b) shows a linear trend ($R^2 = 0.89$), independent of the binder used for the concrete. For reference, the predicted moduli from the Indian standards (IS 456-2000 [41]) and FIB Model Code 2010 [42] are also plotted.

#### 3.1.2. Shrinkage

The autogenous and drying shrinkage influences cracking in concrete structures, as the binder phase continuous to deform amidst the restraint offered by the aggregates in the hardened concrete. Autogenous shrinkage is controlled by the change in the internal RH (due to consumption of free water) of the system due to self-desiccation at lower water-binder ratio, whereas the loss of moisture (due to drying) from the concrete leads to drying shrinkage. Bissonnette et al. [43] reported that the influencing parameters affecting the shrinkage measurement were water- binder ratio, size of specimen, relative humidity, and paste volume. A more detailed classification of factors is listed in [44].

The evolution of shrinkage strains in cylindrical and prismatic specimens is given in Figs. 4–6. The autogenous shrinkage strains measured for all the concretes were lower compared to the values reported in literature [45]. In this study, the specimens were wrapped with aluminum adhesive tape only after 28 days of curing. The autogenous shrinkage from casting until 28 days ($t_o$) is neglected in this measure-

**Table 3**
Mix designs of the different concretes considered in this study.

| Concrete set | Grade | Mix I.D. | w/b | Cement | Fly ash | Water | Fine aggregate | Coarse aggregate | | Unit weight | SP[a] | Paste volume | Slump |
|---|---|---|---|---|---|---|---|---|---|---|---|---|---|
| | | | | | | | | 10 mm | 20 mm | | (% by wt. of binder) | Litres/m$^3$ | (mm) |
| | | | | kg/m$^3$ | | | | | | | | | |
| 1 | M30 | OPC M30 | 0.5 | 310 | 0 | 155 | 695 | 496 | 744 | 2371 | 0.02 | 253.1 | 100 |
| | | FA30 M30 | 0.45 | 217 | 93 | 139.5 | 723 | 491 | 737 | 2414 | 0.65 | 245.5 | 100 |
| | | LC3 M30 | 0.5 | 310 | 0 | 155 | 708 | 491 | 736 | 2487 | 1 | 258.0 | 80 |
| 2 | M50 | OPC M50 | 0.4 | 360 | 0 | 144 | 703 | 477 | 716 | 2385 | 0.65 | 257.9 | 90 |
| | | FA30 M50 | 0.35 | 266 | 114 | 133 | 699 | 475 | 713 | 2406 | 0.6 | 263.0 | 120 |
| | | LC$^3$ M50 | 0.4 | 340 | 0 | 136 | 704 | 488 | 732 | 2463 | 0.85 | 249.0 | 120 |
| 3 | Common mix (C mix) | OPC – C mix | 0.45 | 360 | 0 | 162 | 721 | 463 | 694 | 2399 | 0.1 | 275.9 | 90 |
| | | FA30 – C mix | 0.45 | 252 | 108 | 162 | 721 | 463 | 694 | 2385 | 0.23 | 285.1 | 90 |
| | | LC$^3$ – C mix | 0.45 | 360 | 0 | 162 | 687 | 476 | 715 | 2414 | 0.36 | 281.6 | 120 |

Note:
[a] SP % denotes the amount of superplasticizer solids (SP content).

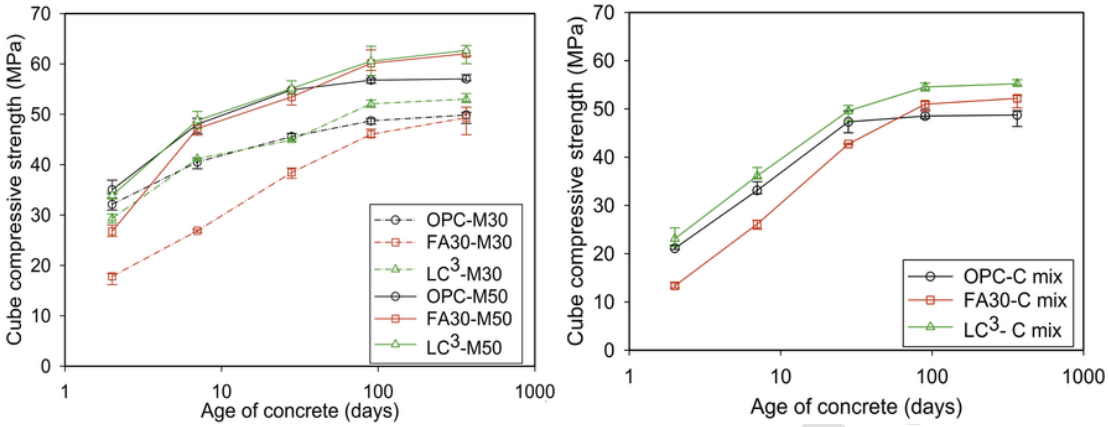


**Fig. 2.** Evolution of Compressive strength in the concrete mixes. (a) M30 concretes and M50 concrete and (b) common mix (C-mix).

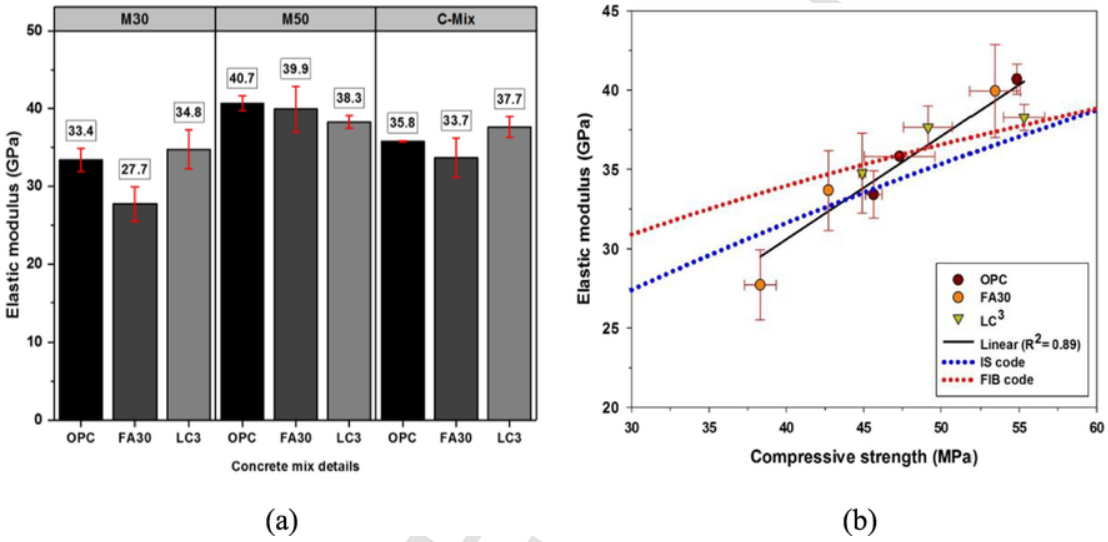


**Fig. 3.** (a) Elastic moduli of concretes made with OPC, FA30, and LC$^3$ and (b) correlation between elastic modulus and compressive strength.

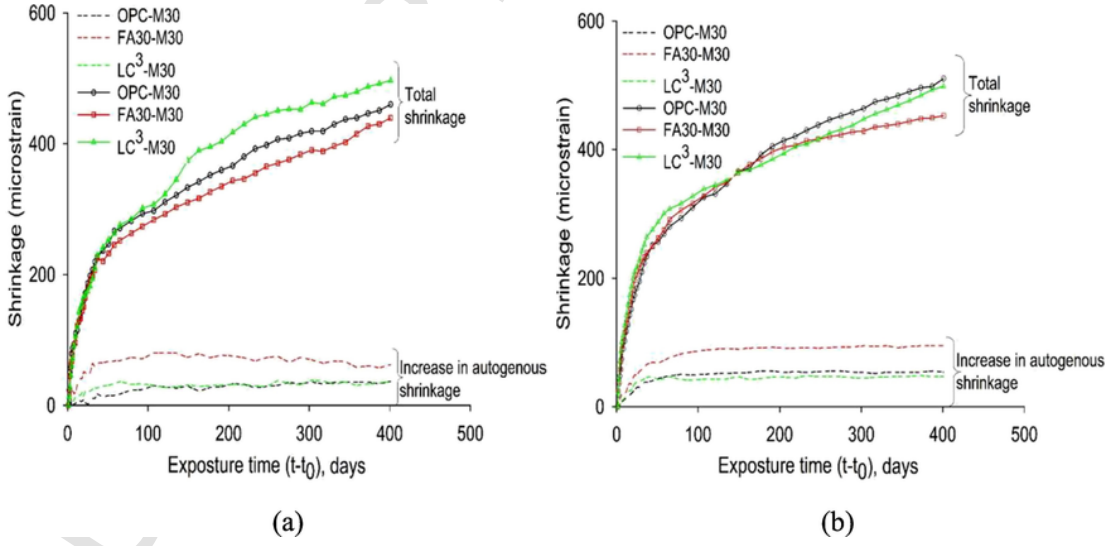


**Fig. 4.** Shrinkage strain in M30 concretes (a) cylindrical specimens and (b) prismatic specimens.

ment. The drying shrinkage is presented (in Figs. 4–6) as total shrinkage as it also includes a part of autogenous shrinkage.

For M30 concrete mixes, the measured autogenous shrinkage strains after 28 days were comparable for the OPC and LC$^3$ systems (Fig. 4). However, FA30 showed a higher shrinkage (autogenous) due to lower water-binder ratio in the concrete mix. In contrast, for the same reason of the lower water content, drying shrinkage results sug-

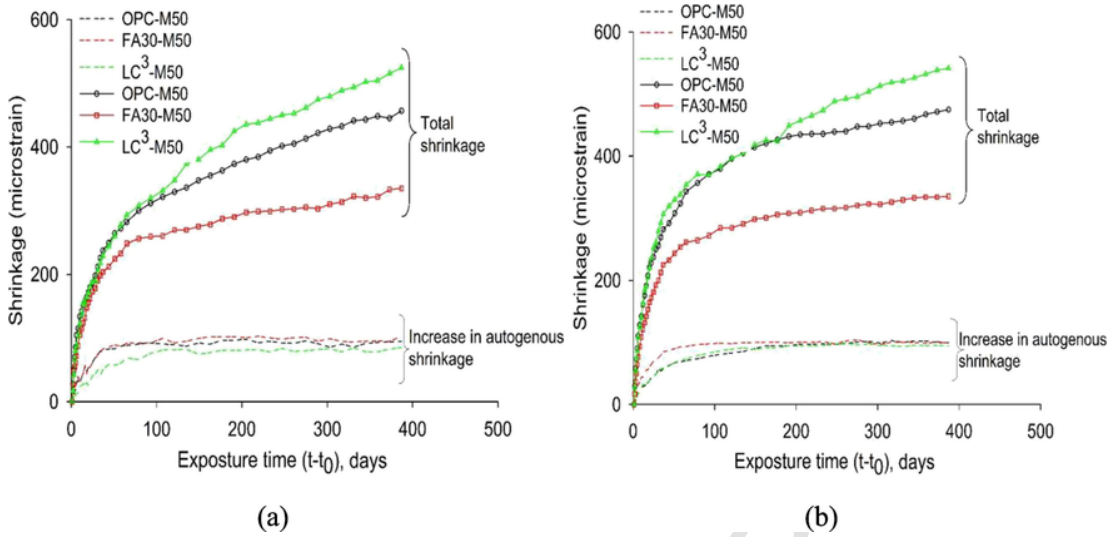


**Fig. 5.** Shrinkage strain in M50 concretes (a) cylindrical specimens and (b) prismatic specimens.

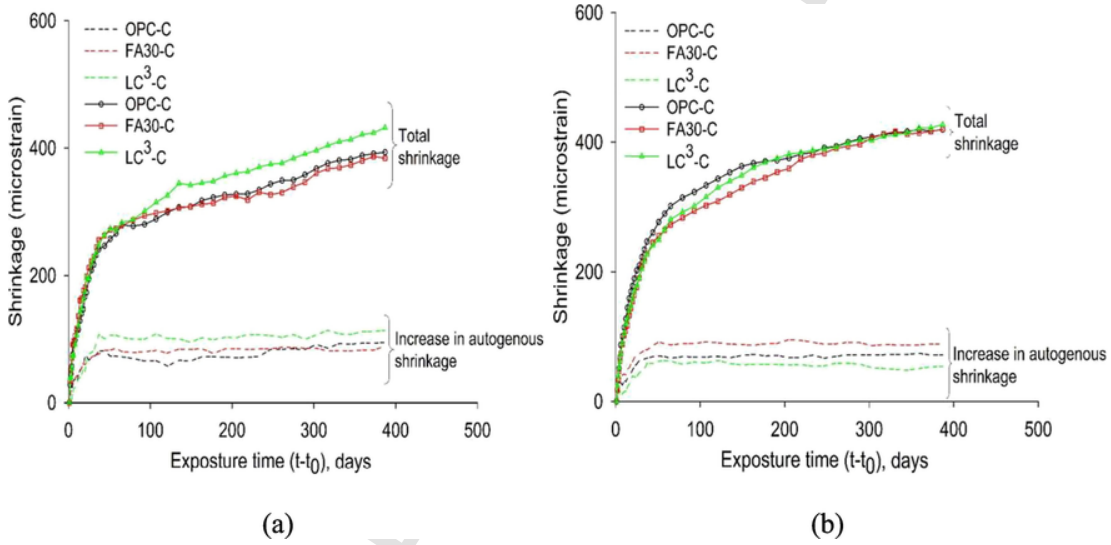


**Fig. 6.** Shrinkage strain in equivalent binder content and w/b concretes (a) cylindrical specimens and (b) prismatic specimens.

gest that FA30 has lower shrinkage than the OPC and $LC^3$ concretes. Fig. 5 reports the results of the M50 grade concretes, and it is seen that the drying shrinkage of FA30-M50 concrete was comparatively lower (than M30 concretes) due to the lower water-binder ratio (0.35) opted for the FA30-M50 concrete mixes. The initial shrinkage of FA30-M50, which occurs at a faster rate was also found to be lower in both types of specimens (Fig. 5a and b). In the C-mix (with the same binder content and w/b), the measured shrinkage strains in the different binder systems were comparable (Fig. 6). From the results, it is seen that the influence of water-binder ratio dominates the effects of shrinkage development in concrete, which is evident from the difference in the shrinkage strains noted in the two sets of equivalent grade concrete mixes. However, the concretes with the same binder content and w/b ratio showed a minimal difference between the different binder systems.

The shrinkage behaviour can be further rationalised by dissociating the effect of water-binder ratio, pore sizes, and degree of hydration at varying water-binder ratio for the three binder systems. The governing mechanisms causing shrinkage in the different cementing matrices are controlled by these factors. First and foremost, a lower water-binder ratio (typically $<0.4$) leads to reduced hydration degree due to a more packed capillary space. This causes a reduction in the amount of hydrates and thereby, the medium which is shrinking in the concrete is also reduced. Alternatively, at lower water-binder ratios, there is an increase in the amount of the finer pores (more specifically in the blended systems) which increases the shrinkage per unit mass loss due to higher capillary pressure during drying.

This difference can be explained by taking a closer look at the shrinkage strain and mass loss of the different binder systems (Fig. 7). The shrinkage performance in fly ash mixes can be attributed to the lower hydration degree, lower water-binder ratios and coarser pores in FA30 systems from the slow reaction of fly ashes which reduces the amount of hydrates. This results in lower shrinkage strain, even at similar amount of mass loss due to drying. In contrast, a higher water content, finer pores (details of pore sizes are discussed in Table 6) and higher hydration extent due to early reactivity of calcined clay in the $LC^3$ systems (M30 and M50 mixes) collectively increases the shrinkage strain (marginally), despite lower or similar amount of mass loss from drying (Fig. 7).

In previous studies on metakaolin addition on shrinkage evolution, Brooks and Johari [46] reported that increasing metakaolin content from 5% to 15% lowered the early age autogenous shrinkage and dry-

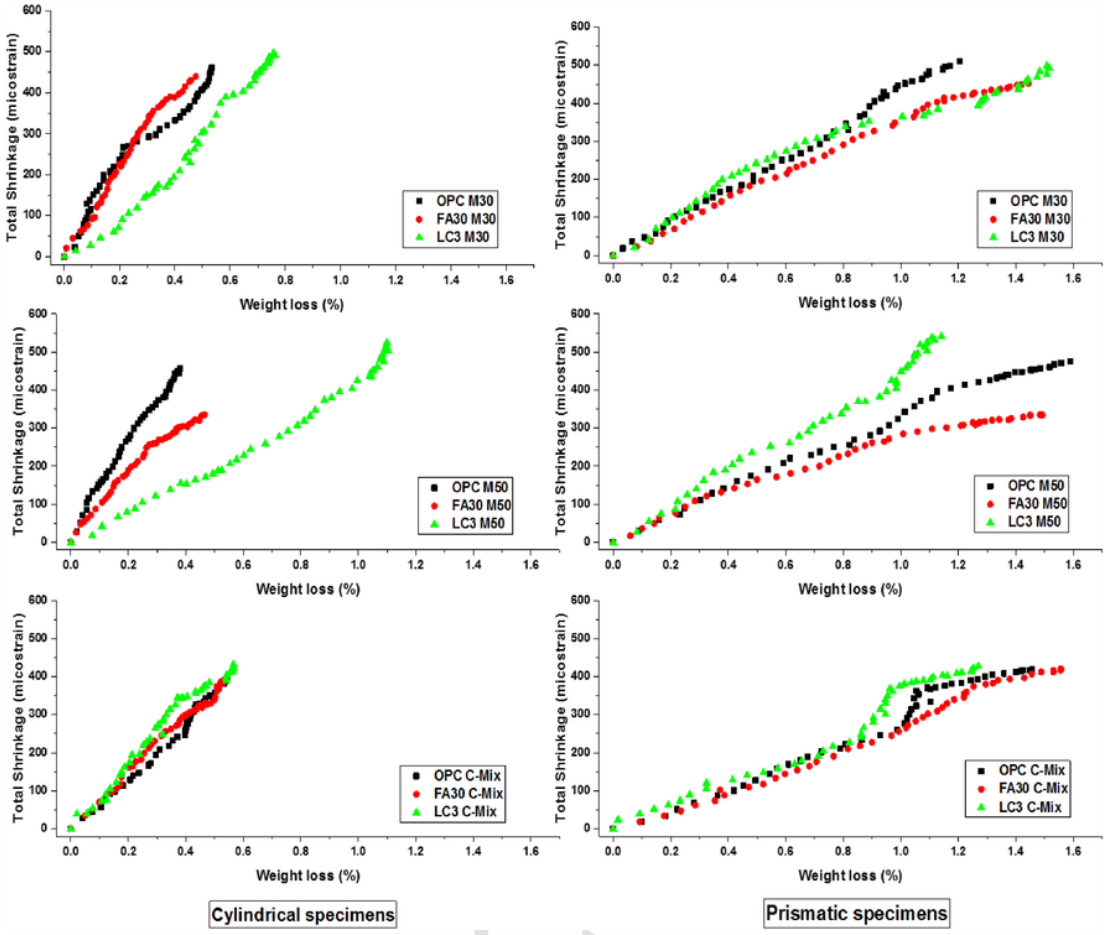


**Fig. 7.** Relationship between total shrinkage and weight loss (%) for the different binder systems (mass losses in the prismatic specimens are higher due to higher surface area).

ing shrinkage, and increased the long term autogenous shrinkage. Metakaolin has been reported to reduce free drying shrinkage [47,48]. Literature on limestone addition also shows that increasing amounts of limestone replacing the Portland cement results in similar (or lower) drying shrinkage for up to 10% substitution [49,50], whereas higher replacement level (20% or above) can lead to increase in the drying shrinkage [51,52]. From this study, it can be concluded that combined substitution of limestone and calcined clay resulted in similar or marginally higher shrinkage in concretes as compared to OPC and FA30. The effect of water-binder ratio (the amount of free water) and mixture proportioning (paste volume) had a more dominant effect on the evolution of shrinkage strains between the different binders.

The measured shrinkage strains and the prediction by existing shrinkage models are summarized in Table 4. From the results, it can be seen that the shrinkage strains predicted by B4 model [53] was nearly consistent with the experimental observation for the three binder systems (except for $LC^3$-M50). FA30 mixes had a higher deviation from the predictions with ACI model [54] and FIB - Model code [42] in all the cases. The deviations were comparatively less in $LC^3$ than FA30 concrete mixes in the equivalent strength category. This is mainly due to the lower water-binder ratio opted for FA30 mixes to achieve the target $28^{th}$ day strength. In the case of C-mix, B4 model could give a closer prediction to the experimental values with the three binder systems.

To explain the difference in the shrinkage performance observed in the three binder systems, the evolution of the total shrinkage strain is plotted against the mass loss observed (as weight loss %) in Fig. 7. It is noted that the maximum weight loss (%), at the drying period of 400 days, was higher in the prismatic specimens than cylindrical specimens. The prismatic specimens have a greater surface area (per unit volume) leading to faster rate of weight loss in these specimens. However, the observed shrinkage strains were similar (or marginally lower in cylindrical specimens) between both the specimens.

In the case of cylindrical specimens, the ultimate weight loss is higher due to higher water-binder ratio and lower binder content in M30 and M50 concrete mixes of $LC^3$ than OPC and FA30. This confirms that the amount of free water predominantly affects the shrinkage development in the equivalent grade concrete mixes, despite the variation in the capillary pressure (which leads to shrinkage) due to difference in the pore sizes. Results also suggest that for the same extent of moisture loss, $LC^3$ binder showed lesser shrinkage at an equivalent strength level. However, the concrete made with similar mixture proportion shows that the mechanism of shrinkage development due to loss of moisture can be similar between concretes made with the three binder systems.

The results of the prismatic specimens suggest that drying was marginally higher for the $LC^3$ concretes in all the categories, which in turn, results in higher shrinkage strain of the $LC^3$ as observed in Table 4.

### 3.2. Durability properties

#### 3.2.1. Resistivity development

Electrical resistivity reflects the interconnectivity of pores in the concrete, and thereby gives a direct indication of the concrete quality with respect to the resistance to ionic ingress. Feliu et al. [56] have shown that the electrical resistivity controls concrete's resistance to

**Table 4**
Comparison of experimentally measured shrinkage with available models.

| Concrete grade | | | M30 | | | M50 | | | C-mix | | |
|---|---|---|---|---|---|---|---|---|---|---|---|
| Binder | | | OPC | FA30 | $LC^3$ | OPC | FA30 | $LC^3$ | OPC | FA30 | $LC^3$ |
| Shrinkage (microstrain) at (1 year) | Cylindrical specimens | | 450 | 430 | 490 | 450 | 330 | 520 | 390 | 380 | 430 |
| | Prismatic specimens | | 500 | 450 | 490 | 470 | 330 | 540 | 420 | 420 | 430 |
| | B4 model [53] | Cylinders | 410 (−40) | 370 (−60) | 410 (−80) | 390 (−60) | 380 (+50) | 360 (−160) | 430 (+40) | 410 (+30) | 430 (0) |
| | | Prisms | 430 (−70) | 390 (−60) | 430 (−60) | 410 (−60) | 400 (+70) | 380 (−160) | 460 (+40) | 420 (0) | 450 (+20) |
| | ACI model [54] | Cylinders | 440 (−10) | 440 (+10) | 430 (−60) | 450 (0) | 480 (+150) | 470 (−50) | 450 (+60) | 450 (+70) | 470 (+40) |
| | | Prisms | 500 (0) | 500 (+50) | 480 (−10) | 500 (−60) | 545 (+215) | 520 (−20) | 500 (+80) | 500 (+80) | 530 (+100) |
| | CEB Fib 2010 model [55] | Cylinders | 471 (+20) | 520 (+90) | 490 (0) | 450 (0) | 440 (+110) | 450 (−70) | 480 (+90) | 490 (+110) | 460 (+30) |
| | | Prisms | 540 (+40) | 600 (+150) | 560 (+70) | 510 (+40) | 500 (+170) | 510 (−30) | 550 (+130) | 560 (+140) | 530 (+100) |

Note: The values in the parenthesis indicate the difference between the experimental and predicted shrinkage strain.

corrosion propagation (power relationship, a linear relationship between corrosion current and resistivity on a log-log scale) and also correlates well with chloride resistance assessed by several techniques [57–59]. The surface resistivity serves as a quick indication of the resistivity of the bulk concrete and is often used a tool for concrete quality and optimization of concrete mixes [57].

Fig. 8 depicts surface resistivity values of all the concrete mixes studied at 28 days, 56 days and 90 days. In all the binder systems, the results indicate that M50 concrete attains higher resistance than M30 concrete mixes. This can be due to lower water-binder ratio in these mixes to produce a higher-grade concrete. However, the $LC^3$ concrete systems attains highest resistivity, irrespective of the range of concrete mixes considered in this study. Early refinement of pore structure in the $LC^3$ system leads to increase in resistivity at early ages against other systems (discussed in detail elsewhere [60]).The resistivity of the FA30 mixes improved only after 28 days indicating the positive impact of the fly ash with extended curing, whereas OPC mixes shows minimal changes in the resistivity with curing duration. This is expected in OPC as clinker phases undergo maximum reaction at an early ages (by 7 days) and there is a slowdown in their contribution with time. The ACI classification [61] on corrosion rate (high, moderate, and low) based on surface resistivity values is indicated in the Fig. 8 to show the relative quality of the different concretes. The results clearly show that the concrete made with $LC^3$ binder can have excellent resistance to corrosion propagation of the embedded steel.

In addition to the ACI classification for corrosion rate, FM5-578 [32] suggests a classification for chloride permeability resistance based on the surface resistivity measurement. The classification includes a wider surface resistivity range (Risk of chloride ingress, given surface resistivity in k.ohm-cm - high: $<12$, moderate: 12–21, low: 21–37, very low: 37–254, and negligible: $>254$). In line with this classification, all the $LC^3$ concretes have negligible chloride ingress (Fig. 9), while fly ash concretes – at later ages – have a very low risk. OPC concretes, on the other hand, have a high to moderate risk of corrosion. Studies on the resistivity development of OPC, FA30 and $LC^3$ cement paste was conducted over a range of water-binder ratios [62] and found that the improved resistivity development in $LC^3$ binder is due to the difference in the kinetics of microstructural development in the binder systems, and also showed a more densified micrographs at 28 days in the $LC^3$ systems. In addition, fly ash showed a steady development of resistivity to reach the $LC^3$ resistivity range (i.e., initial value of $LC^3$) in concretes only after 1 year of curing. This difference in the behaviour suggests that the performance of $LC^3$ systems is strongly influenced by calcined clay's early reactivity potential which leads to a refined pore structure and densified cementing matrix, thereby causing a higher electrical resistance in concretes with $LC^3$ binder.

### 3.2.2. *Resistance to chloride ingress*

The total charge passed in the RCPT gives an indirect estimate of the chloride resistance of the concrete. Lower charge passed implies higher resistance to chloride ingress. A detailed classification of concrete quality based on the charged passed is available in ASTM C1202 [34]. Though the test has been prone to several criticisms, it is still widely adopted for the evaluation of the concrete quality (especially chloride resistance of concrete) in worldwide construction practices. A recent study by Dhanya and Santhanam [59] has reemphasised on the credibility of this test method for evaluation of chloride resistance of concretes with Supplementary Cementitious Materials. The experimental results for the nine concrete mixes at 28 days and 90 days are presented in Fig. 9. This result shows that concrete made with $LC^3$ binder have a minimal amount of total charge passed at both 28 days and 90 days, signifying excellent resistance to chloride ingress in these concrete systems at an early age (28 days). The FA30 mixes showed major improvement in the performance only with extended curing age i.e., at 90 days. The qualitative classification of concrete quality based on ASTM C1202 suggest that fly ash produces excellent quality of concrete only after extended curing while $LC^3$ attains much better resistance at relatively early age. Irrespective of the different concrete mixtures, the RCP values of the $LC^3$ concrete mixes were found to be in the 'Negligible' charge passed category. The major reason is due to the refined pore structure attained at early ages in the $LC^3$. In addition, the calcined clay contains more reactive aluminates, which can lead to more chloride binding compared to other systems due to the difference in the

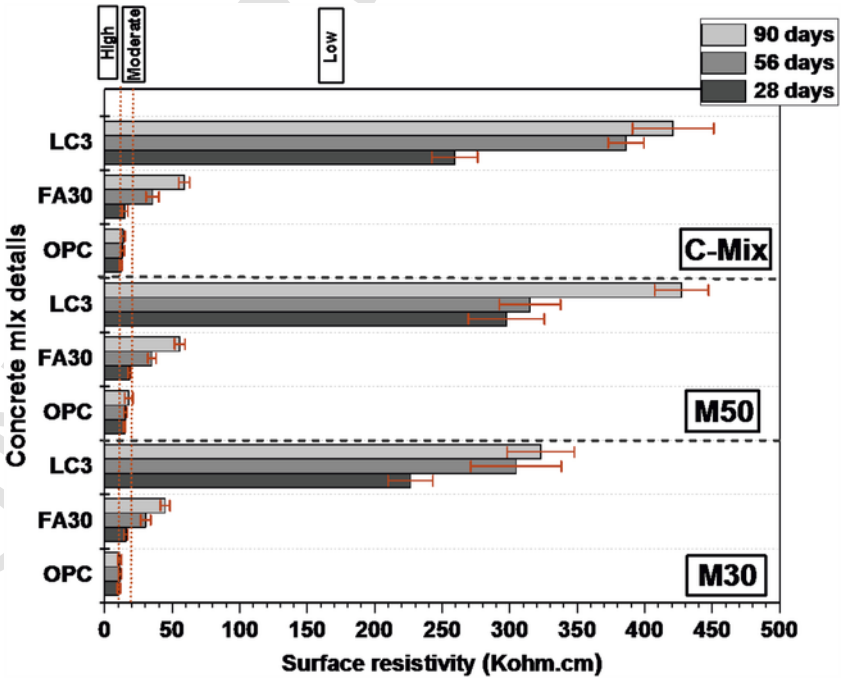


**Fig. 8.** Surface resistivity of the different concretes at 28 days, 56 days and 90 days (the corrosion propagation rate classification from ACI 222R-01 suggests that $LC^3$ concrete systems can have excellent corrosion resistance).

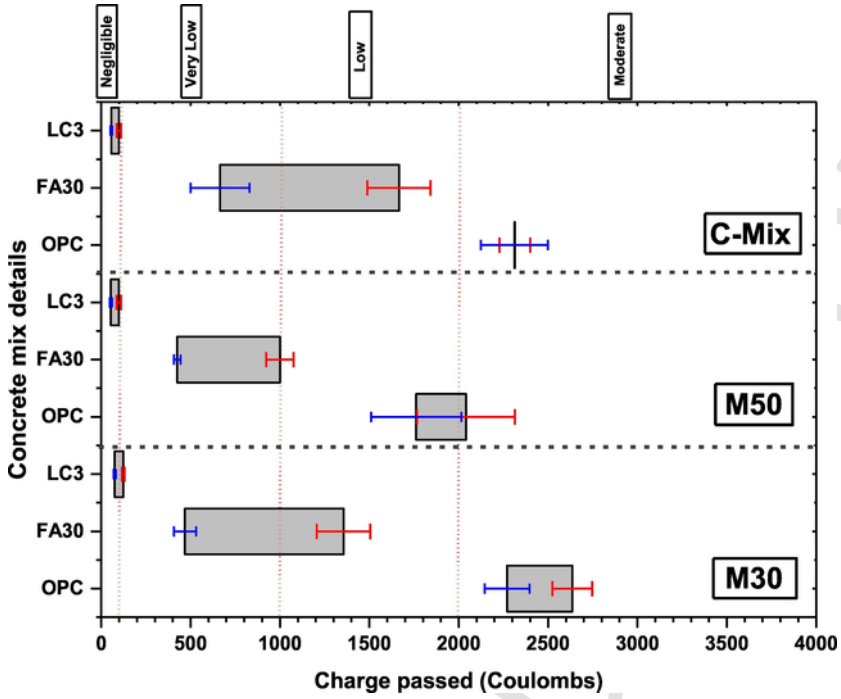


**Fig. 9.** RCPT - total charge passed in the different concretes at 28 days (red) and 90 days (blue). (For interpretation of the references to colour in this figure legend, the reader is referred to the web version of this article.)

hydration products (details on the difference in microstructure discussed in Section 4).

In addition to the RCP test, Chloride migration test was also considered to obtain a quantitative measure of the chloride resistance as migration coefficient i.e., the rate of chloride ingress under applied external potential. The results of non-steady state chloride migration coefficient at 28 days and 90 days, presented in Fig. 10, are affirmative of the RCPT results. The addition of fly ash lowers the chloride migration coefficient by 40–50% at 28 days, and nearly 70–80% at 90 days compared to the OPC in different categories of concretes. In concretes made with the $LC^3$ binder, the chloride resistance had improved by nearly 80–90% (with respect to OPC) by 28 days in all the categories considered. This signifies the excellent resistance of $LC^3$ binder to chloride ingress at an early age. For the chloride migration test, the qualitative classification was adopted from the recommendation in RILEM TC 230-PSC [63]. In the concretes evaluated in this study, the M30 con-

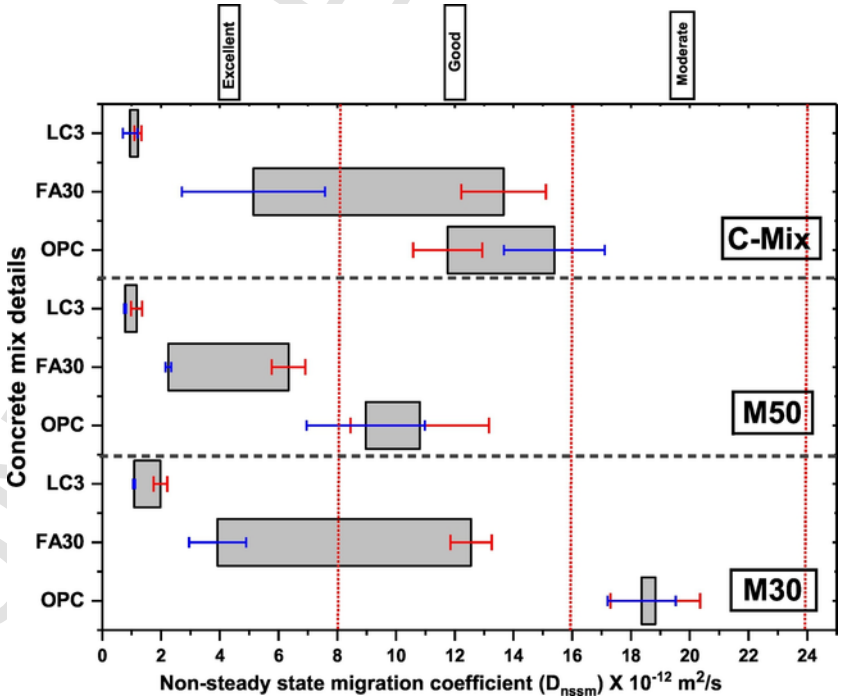


**Fig. 10.** Chloride migration coefficient of the different concretes at 28 days (red) and 90 days (blue). (For interpretation of the references to colour in this figure legend, the reader is referred to the web version of this article.)

cretes with the OPC and fly ash attain moderate and good resistance to chloride penetration. In M50 grades, fly ashes also attain excellent resistance to chloride migration. In all the category of concretes, $LC^3$ systems attain excellent resistance to chloride ingress. It is also interesting to note that in the case of FA30 and $LC^3$ concrete mixes, the mixes with higher water-binder ratio (for instance, FA30-M30 and FA30-C mix with w/b ratio of 0.45 each) had greater enhancement in the performance than mixes with lower water-binder ratio (FA30 M50 with w/b ratio of 0.35). This can be clearly noticed in Fig. 9 in which the shift in the bar indicates improvement in the charge passed of different concrete mixes from 28 days to 90 days. Though similar trends were noticed with the $LC^3$ binder system, the absolute values attained in $LC^3$ concrete mixes were much lower than FA30. It can be concluded that traditional description of durability as a function of the water-binder ratio can be overlooked in presence of pozzolans (more in the case of high performance pozzolans such as calcined clays) which leads to continuous enhancement of properties with appropriate curing. And the potential for performance enhancement (with respect to chloride penetration resistance) due to SCMs can be significantly higher for concretes with higher water-binder ratio.

The total charge passed in the RCPT has a strong correlation with the non-steady state migration coefficient estimated from the chloride migration experiment (Fig. 11), confirming the credibility of evaluation of the chloride resistance of the different binder systems by two different techniques. Also, the relationship between surface resistivity and RCPT charge passed conforms to the established correlations presented in literature [58,59,64–66].

### 3.2.3. Gas permeability

The Oxygen Permeability Index (OPI) obtained as the negative log of the Darcy's permeability coefficient is presented in Fig. 12. Alexander et al. showed that OPI has a direct correlation with the carbonation rate for specific binder systems [67]. It is also necessary to understand that carbonation can be influenced by calcium buffering capacity in addition to gas permeability. Within a particular binder system, the latter will have a predominant influence on the carbonation resistance,

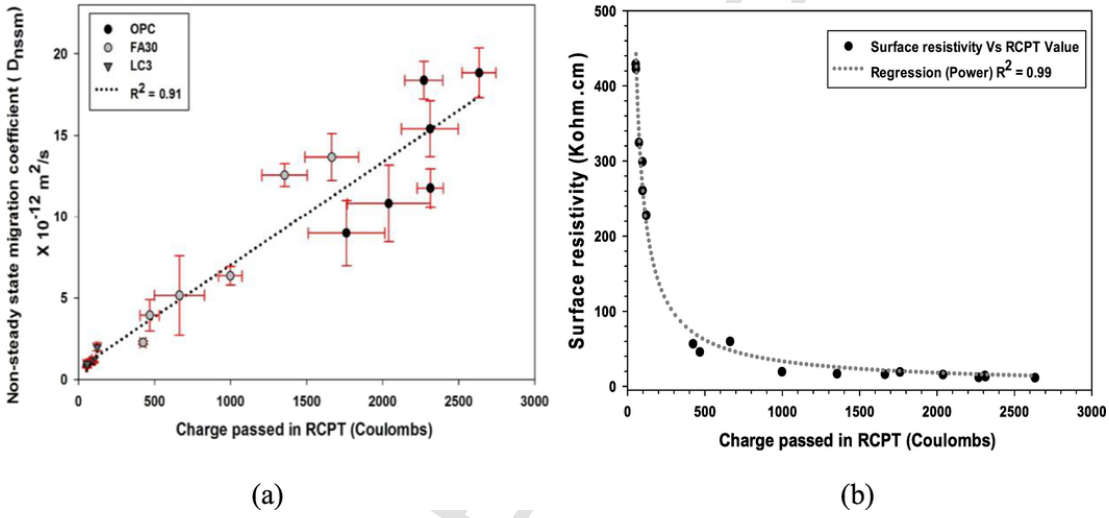


**Fig. 11.** a) Chloride penetration resistance of different binders evaluated by RCPT and ACMT, and b) correlation between surface resistivity and charge passed in RCPT.

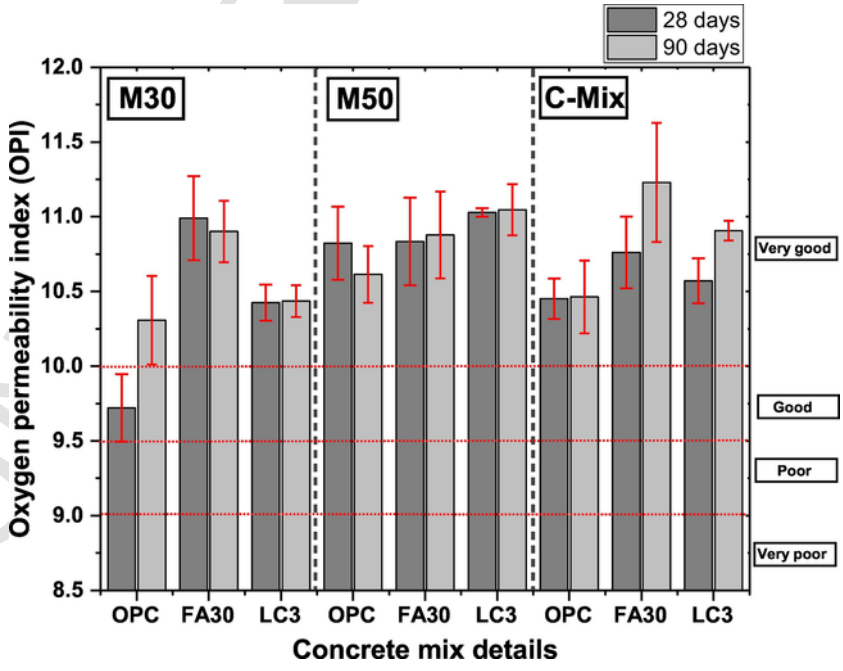


**Fig. 12.** Gas permeability (presented as OPI) of the different concretes at 28 days and 90 days. Note that the value in the Y-axis is –'ve log of permeability coefficient k.

whereas, between different binder systems, the former will control the performance. The results show that all concretes considered in the study had low permeability as per the classification (i.e., excellent permeability resistance category) suggested by Alexander et al. [68]. The results suggest that both FA30 and $LC^3$ attain higher gas permeability resistance than OPC. Notably, M50 concretes attain higher resistance than M30 grade of concrete within a particular binder system due to better concrete mix design. At equivalent strength (M30), FA30 mixes attain higher resistance than $LC^3$. However, w/b ratio was lowered in the FA30 mixes to produce equivalent strength concrete, as against OPC and $LC^3$. Between the M50 concrete mixes, permeability indices of FA30 and $LC^3$ were comparable, despite the lower water-binder adopted in the FA30 mixes. In addition, the range of values obtained in $LC^3$ had a lower variability (within the 4 specimens tested in this case) than OPC and FA30, resembling a better quality of concrete (i.e., homogeneity) against gas permeability with $LC^3$. The C-mix with equivalent binder content and water-binder ratio shows higher OPI in FA30 and $LC^3$ than concrete made with OPC.

### 3.2.4. Sorption and porosity

Concrete's resistance to moisture ingress by capillary absorption is commonly evaluated by the absorption rate in concrete represented as sorptivity. Fig. 13 shows the sorptivity index of the concretes. The qualitative classification of the concrete based on sorptivity from Alexander et al. [68] is used here to classify the concretes. Due to SCM addition, the combined pozzolanic and filler effect leads to more tortuous pores and reduces adsorption rate in FA30 and $LC^3$ concrete mixes. The results show that concretes with $LC^3$ and FA30 binders attain lower Sorptivity index than OPC concrete in M30 and C-mix. All concrete in the M50 strength grade fall into the same classification category (good) with respect to sorptivity. It is noteworthy to mention that $LC^3$ concretes, at a similar binder content (i.e., for the C-mix) showed significantly lower sorptivity values. This confirms the improvement in the resistance to capillary adsorption with the $LC^3$ binder system.

The specimens after the sorptivity test were used to estimate the water accessible porosity by vacuum saturation method. The results are summarized in Table 5. The water accessible porosity was found to vary partially in accordance with the water-binder ratio. The water accessible porosity is more representative of the bulk concrete mixture covering a major part of macro-voids, more specifically the entrapped air porosity and part of the saturated porosity of the cement paste matrix of the concrete [39]. In terms of the bulk porosity, the expected porosity changes with age are minimal, as the pore refinement due to SCMs will occur in the capillary pore space of the binder matrix.

For a detailed understanding of the evolution of pore structure and the capillary pore space in the three binder systems, porosimeter studies were also conducted on the concrete samples at 28 days and 90 days.

In addition to the water accessible porosity, small chunks of concrete were sampled from the centre of concrete cubes for mercury intrusion porosimetry studies. Though the total intruded volumes were higher in the concretes with $LC^3$, the critical pore size was significantly lower than both OPC and FA30 concretes at 28 days (Table 6). From 28 days to 90 days, the shift in the pore sizes was minimal in the case of OPC and $LC^3$. However, the pore diameters of $LC^3$ were lower compared to OPC. In contrast, the FA30 concrete mixes showed a better reduction of the pore sizes from 28 days to 90 days. This clearly indicates a refinement of the pore structure with $LC^3$, which explains the supe-

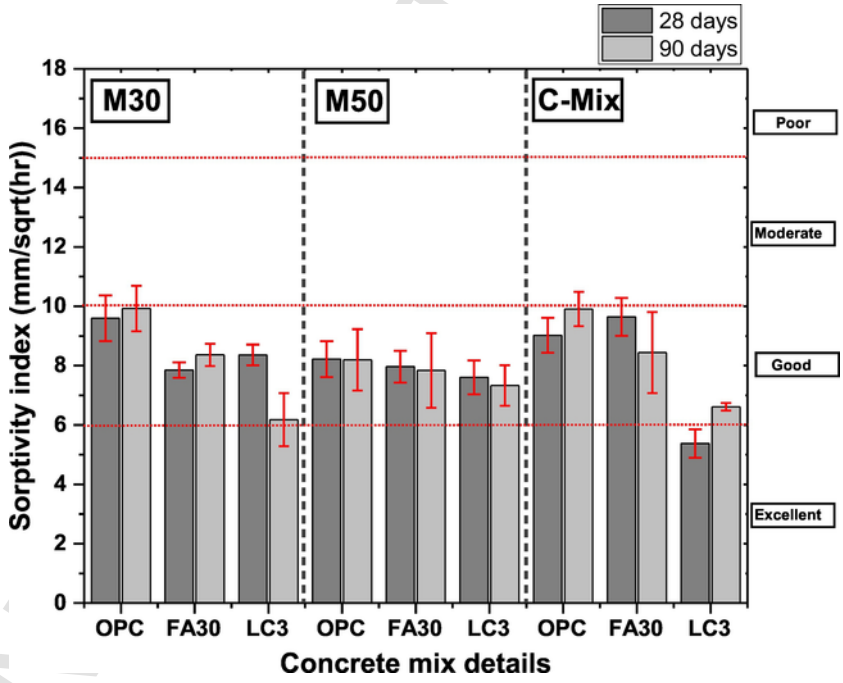


**Fig. 13.** Water sorptivity of the different concrete at 28 days and 90 days.

**Table 5**
Measure of water accessible porosity (mass, %) of the concrete mixes.

| Concrete grade | M30 | | | M50 | | | C-mix | | |
|---|---|---|---|---|---|---|---|---|---|
| Age\binder | OPC | FA3 | $LC^3$ | OPC | FA30 | $LC^3$ | OPC | FA30 | $LC^3$ |
| 28 days | 7.6±0.3 | 8.3±0.4 | 10.0±0.1 | 6.2±0.3 | 6.9±0.4 | 5.2±0.4 | 7.3±0.1 | 6.9±0.2 | 9.7±0.7 |
| 90 days | 8.8±0.5 | 8.4±0.3 | 9.8±0.7 | 7.2±0.1 | 8.5±0.7 | 6.6±0.6 | 7.9±0.3 | 2.9±0.1 | 8.4±1.4 |

**Table 6**
Porosimetry results of concrete samples at 28 and 90 days.

| Concrete mixes | M30 | | | M50 | | | C-mix | | |
|---|---|---|---|---|---|---|---|---|---|
| | OPC | FA30 | $LC^3$ | OPC | FA30 | $LC^3$ | OPC | FA30 | $LC^3$ |
| Intruded pore volume ($mm^3/g$) at 28 days | 85.11 | 92.40 | 77.31 | 66.45 | 77.67 | 83.57 | 58.85 | 95.08 | 72.89 |
| Intruded pore volume ($mm^3/g$) at 90 days | 54.89 | 53.49 | 48.90 | 37.49 | 50.27 | 53.70 | 33.43 | 41.14 | 59.03 |
| Critical pore size (diameter, in nm) at 28 days | 41.1 | 31.6 | 24.4 | 32.7 | 43.8 | 16.4 | 74.0 | 41.3 | 20.4 |
| Critical pore size (diameter, in nm) at 90 days | 31.9 | 20.8 | 17.3 | 23.0 | 14.9 | 23.4 | 74.5 | 18.33 | 19.8 |

rior performance in the durability tests. Further, the higher intruded volume matches with the result of the higher water accessible porosity of these systems.

## 4. $LC^3$ binder system for structural concrete

The environmental concerns associated with the cement production mainly with respect to resource utilization and $CO_2$ emission is driving the need for more sophisticated binder systems. This study described the performance of the concrete systems made with one such binder system involving calcined clay and limestone. Based on the results of the study, it is understood that the use of $LC^3$ brings about perceptible benefits to the durability properties of concrete, considered here in terms of the resistance to chloride, moisture, and gas penetration.

The deterioration mechanisms associated with each service condition are different and hence, performance based design approaches of concrete should consider parameters specific to a condition. Dhanya and Santhanam [66] proposed a combined classification system for chloride environments (specifically the sea water category – XS as per EN 206 [69]) where a combination of durability indicators was suggested for each service condition. This can ensure an appropriate selection of concrete mixes for a given service environment. The service conditions and proposed set of concrete parameters for a chloride-laden environment are given in Tables 7 and 8. The 28- and 90-days results from the study are also presented in the same table. The concrete mixes meeting the desired durability requirement among the nine concrete mixes are identified and highlighted in green colour. From the data shown in the tables, it is apparent that mixes with $LC^3$ binder were suitable for all three exposure conditions at 28 days. On the other hand, the fly ash mixes met the required specifications only after extended curing (i.e., 90 days in this case) except FA30-M50 mix which satisfied the RCPT criterion by 28 days. It is interesting to note that concretes made with OPC hardly met the performance requirements for chloride laden exposure conditions. This confirms the necessity of using SCMs as clinker replacement in the marine environment.

From the results of this study, it is clear that the $LC^3$ binder system has the potential to produce high-performance concrete for the marine environment without any ultrafine supplementing additives like silica fume or metakaolin etc., as required in the case with fly ash concrete mixes. One of the major driving factors for this performance is the microstructure attained in these systems. The composition of the inner

**Table 7**
Suitability of concretes for the marine environment (using limiting values suggested by [35]) at 28 days.

| Service conditions | Mechanisms | Strength (MPa) | Durability Parameters (28 days) | | | | | | | | |
|---|---|---|---|---|---|---|---|---|---|---|---|
| | | | Wenner Resistivity | | | Total charge passed from RCPT | | | Sorptivity (mm/sq·hr) | | |
| Exposed to airborne salt but in direct contact with sea water | Diffusion, sorption, physical degradation | 40 | 50–100 | | | <2000 | | | 6 to 10 | | |
| XS1 | | | OPC | FA30 | $LC^3$ | OPC | FA30 | $LC^3$ | OPC | FA30 | $LC^3$ |
| | M30 | Mix-1 | 11.1 | 16.4 | 227.5 | 2635 | 1356 | 123 | 9.6 | 7.6 | 8.4 |
| | M50 | Mix-2 | 16.4 | 19.0 | 298.6 | 2040 | 1000 | 98 | 8.2 | 8.0 | 7.6 |
| | C-Mix | Mix-3 | 12.6 | 15.7 | 260.4 | 2314 | 1666 | 99 | 9.02 | 9.6 | 5.4 |
| Permanently submerged in sea water | Diffusion, Permeation | 35 | 50–100 | | | <2000 | | | – | | |
| XS2 | | Mix-1 | 11.1 | 16.4 | 227.5 | 2635 | 1356 | 123 | 9.6 | 7.6 | 8.4 |
| | | Mix-2 | 16.4 | 19.0 | 298.6 | 2040 | 1000 | 98 | 8.2 | 8.0 | 7.6 |
| | | Mix-3 | 12.6 | 15.7 | 260.4 | 2314 | 1666 | 99 | 9.02 | 9.6 | 5.4 |
| Tidal, Splash and Spray zones | Diffusion, sorption, Wick action, Permeation, Physical degradation | 50 | >100 | | | <1000 | | | <6 | | |
| XS3 | | Mix-1 | 11.1 | 16.4 | 227.5 | 2635 | 1356 | 123 | 9.6 | 7.6 | 8.4 |
| | | Mix-2 | 16.4 | 19.0 | 298.6 | 2040 | 1000 | 98 | 8.2 | 8.0 | 7.6 |
| | | Mix-3 | 12.6 | 15.7 | 260.4 | 2314 | 1666 | 99 | 9.02 | 9.6 | 5.4 |

**Table 8**
Suitability of concretes for the marine environment (using limiting values suggested by [35]) at 90 days.

| Service conditions | Mechanisms | Strength (MPa) | Durability Parameters (90 days) | | | | | | | | |
|---|---|---|---|---|---|---|---|---|---|---|---|
| | | | Wenner Resistivity | | | Total charge passed from RCPT | | | Sorptivity (mm/sq.hr) | | |
| Exposed to airborne salt but in direct contact with sea water | Diffusion, sorption, physical degradation | 40 | 50–100 | | | <2000 | | | 6 to 10 | | |
| XS1 | | | OPC | FA30 | $LC^3$ | OPC | FA30 | $LC^3$ | OPC | FA30 | $LC^3$ |
| | M30 | Mix-1 | 11.5 | 45.4 | 324.1 | 2271 | 469 | 76 | 9.9 | 8.4 | 6.2 |
| | M50 | Mix-2 | 18.6 | 56.3 | 428.6 | 1762 | 425 | 54 | 8.2 | 7.8 | 7.3 |
| | C-Mix | Mix-3 | 14.1 | 59.5 | 422.3 | 2312 | 665 | 57 | 9.9 | 8.4 | 6.6 |
| Permanently submerged in sea water | Diffusion, Permeation | 35 | 50–100 | | | <2000 | | | – | | |
| XS2 | | Mix-1 | 11.5 | 45.4 | 324.1 | 2271 | 469 | 76 | 9.9 | 8.4 | 6.2 |
| | | Mix-2 | 18.6 | 56.3 | 428.6 | 1762 | 425 | 54 | 8.2 | 7.8 | 7.3 |
| | | Mix-3 | 14.1 | 59.5 | 422.3 | 2312 | 665 | 57 | 9.9 | 8.4 | 6.6 |
| Tidal, Splash and Spray zones | Diffusion, sorption, Wick action, Permeation, Physical degradation | 50 | >100 | | | <1000 | | | <6 | | |
| XS3 | | Mix-1 | 11.5 | 45.4 | 324.1 | 2271 | 469 | 76 | 9.9 | 8.4 | 6.2 |
| | | Mix-2 | 18.6 | 56.3 | 428.6 | 1762 | 425 | 54 | 8.2 | 7.8 | 7.3 |
| | | Mix-3 | 14.1 | 59.5 | 422.3 | 2312 | 665 | 57 | 9.9 | 8.4 | 6.6 |

and outer CSH was evaluated by performing EDS spot analyses over 200 points. The results from Backscattered Scanning Electron Microscopy with Energy Dispersive Spectroscopy (SEM-EDS) study (similar to the method presented in [70]) on pastes (with w/b ratio of 0.40) cured in sealed condition for a period of 150 days are shown in Fig. 14. A distinct difference in the final composition of the microstructure formed in the $LC^3$ system is noted as compared to the OPC or fly ash systems. The CSH (or CASH) composition of the binders shown in the ternary charts indicates an increased amount of silica and alumina in the $LC^3$ binder. Inner C(A)SH in all the binder systems shows uniform more defined composition; outer C(A)SH region shows more variation due to pozzolanic CSH along with an intermixing of other phases such as portlandite, AFt, and AFm. Both inner and outer CSH show a shift in the composition for FA30 and $LC^3$ as compared to OPC. This is due to the availability of pozzolanic components (reactive silica and alumina) from fly ash and calcined clay in the system. However, the change in composition is more significant in the composition of $LC^3$ than FA30. The inner CSH results indicate that the composition shows a greater shift towards incorporating more aluminates available from the calcined clay, denoting the increased availability of the Al and Si for reaction at an early hydration period in the $LC^3$ systems.

The C/S ratio of the inner CSH (CASH) of $LC^3$ was 1.53(±0.15), as opposed to 2.09 (±0.14) and 1.75 (±0.10) in the OPC and FA30 respectively. The increase in reactive alumina content from calcined clay lowered the C/(S + A) to 1.21 (±0.14) in the $LC^3$ system. In OPC and FA30, the ratio of C/(S + A) was nearly 1.95 (±0.13) and 1.60 (±0.09) respectively. The outer CSH composition shows intermixing of the CSH

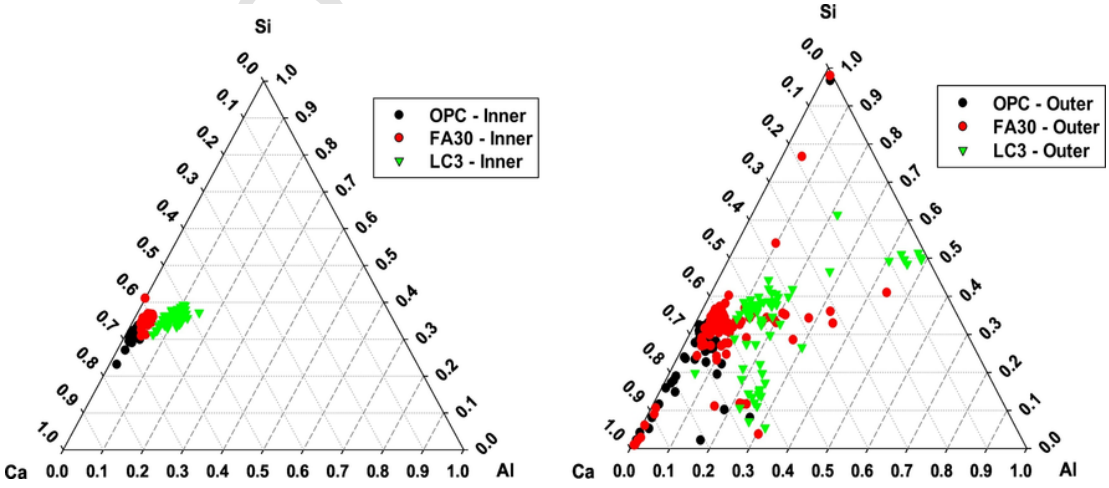


**Fig. 14.** Composition of inner and outer CSH in the OPC, FA30, and $LC^3$ cementitious systems at 150 days.

from the pozzolanic reaction and AFm phase, and traces of unreacted SCMs. An increase in the scatter points towards Ca-Al region is also noted. This can be due to the higher amount of AFt and AFm phases formed in these systems [8]. This change in the chemical composition could be the reason for refined capillary pore space with a more compact microstructure due to the difference in the nature of the hydration products. It is also necessary to acknowledge the fact that the discontinuation of the capillary pores can occur due to the increase in the finer particle fractions (limestone and calcined clay particles) in the $LC^3$ system. However, it is widely acknowledged that there is a difference in the characteristics of CSH based on the density states [71–73]. The difference in the CSH state (high density and low density) can influence the packing density, dispersion state and local stiffness. This implies that the compositional difference also has a significant role in explaining the rate of microstructural development and reduction of capillary pore space in the different binders with curing. The compositional difference demonstrates the impact of high reactivity of the calcined clay present in $LC^3$ binder on the microstructure, leading to a more progressive refinement of pore structure (as presented in Table 6 and [60]). Studies on SEM micrographs [62] showed a denser cementing matrix which was further supported with a refined pore structure of the cement paste in MIP. In terms of the difference in mechanisms between the binder systems, these results put forth the connect between the calcined clay reactivity and the distinct difference in the microstructure development of the $LC^3$ concretes. The early reduction in the capillary pore space has a dominant influence on concrete performance. This can be seen from early increase in the electrical resistivity of the concrete with $LC^3$ (discussed in section: Resistivity development) and transport properties of concrete (discussed in section: Resistance to chloride ingress). The resistivity of the $LC^3$ concrete was significantly higher compared to the FA30 mixes which is mainly due to the fact that there is early refinement (reduction in pore sizes) of the pore space in the $LC^3$ at equivalent age compared to the FA30 mixes [60]. This can partly be attributed to the higher reactivity of calcined clay, which accelerates microstructure development. The fact that the concretes made with $LC^3$ binder could show similar gas permeability and sorptivity value even with higher water-binder ratio compared to FA30 mixes (in M30 and M50 category), and higher resistance in the transport parameters in the common mix category, shows the major positive effect of the microstructure formed in $LC^3$ binder system on the concrete performance.

## 5. Conclusions

Based on the experimental studies conducted on a wide range of properties including mechanical properties, shrinkage, and durability parameters of OPC, FA30, and $LC^3$ concrete mixes, the following conclusions can be drawn:

1. Concretes made with $LC^3$ binder shows comparable strength development characteristics with OPC and better strength development than FA30 in all the concrete mixes. In addition, the amount of binder required to produce higher grade concrete (M50) mixture was lesser with the $LC^3$ binder than in OPC and FA30 concrete mixture. With similar mixture proportion, concrete made with $LC^3$ produces better compressive strengths at all the ages up to 1 year.
2. The elastic modulus in concrete made with $LC^3$ was comparable with the other conventional binder systems. The study on shrinkage showed marginally higher shrinkage strains with $LC^3$ concretes than other binders. However, this can be attributed to higher water-binder ratio adopted for the $LC^3$ concretes with respect to the FA30 concrete mixtures. There was no difference in shrinkage evolution for concretes prepared with the same binder content and w/b.
3. Concrete made with $LC^3$ attains significantly higher resistivity than OPC and FA30 concrete mixtures. This also results in better resistance against ingress of chloride ions which was assessed by RCPT and ACMT. Unlike concrete mixes with fly ashes that show improved durability at an extended curing age of 90 days, the superior performance of $LC^3$ mixtures is noticed by 28 days itself. The result clearly indicates the improved performance of $LC^3$ without the need for any extended curing.
4. The performance against gas permeability and capillary water absorption suggests than $LC^3$ can give better performance with respect to OPC and comparable performance to FA30 with respect to these transport mechanisms. Concretes made with $LC^3$ binder can be ideal for various service environments, and specifically for the marine environment as shown in this study.
5. SEM-EDX analysis showed a distinctly different microstructural composition in the $LC^3$ binder compared to the OPC and FA30, which signifies the difference in the microstructural development of such systems. Furthermore, porosimetry results reveal an early reduction in the pore sizes with the $LC^3$. This results in an early enhancement of durability parameters for concretes with $LC^3$ binder.

This study demonstrates the potential for use of $LC^3$ binder for structural concrete. The results suggest that $LC^3$ can be a high-performance binder system with similar structural properties (Elastic moduli and shrinkage strains) for concreting applications, especially in a chloride laden environment. A detailed investigation of carbonation and sulfate resistance is necessary for adoption of $LC^3$ in various critical service conditions. Further, the resistance to acid attack and frost also needs to be assessed.

## Acknowledgement

The authors would like to acknowledge the financial support from the Swiss Agency for Development and Cooperation (SDC) for the study. Department of Science and Technology and Funds for Improvement of Science and Technology (FIST) Infrastructure grants from Government of India are also gratefully acknowledged. Prof. K. Scrivener, EPFL, Lausanne, Switzerland is thanked for the access to SEM facilities used for EDX analysis reported in this study.

## References

[1] B. Lothenbach, K. Scrivener, R.D. Hooton, Supplementary cementitious materials, Cem. Concr. Res. 41 (2011) 1244–1256, https://doi.org/10.1016/j.cemconres.2010.12.001.
[2] M.C.G. Juenger, F. Winnefeld, J.L. Provis, J.H. Ideker, Advances in alternative cementitious binders, Cem. Concr. Res. 41 (2011) 1232–1243, https://doi.org/10.1016/j.cemconres.2010.11.012.
[3] M. Schneider, M. Romer, M. Tschudin, H. Bolio, Sustainable cement production—present and future, Cem. Concr. Res. 41 (2011) 642–650, https://doi.org/10.1016/j.cemconres.2011.03.019.
[4] D.P. Bentz, Powder additions to mitigate retardation in high-volume fly ash mixtures, ACI Mater. J. 107 (2010) 508–514.
[5] A.C. Emmanuel, P. Haldar, S. Maity, S. Bishnoi, S. Maity, Second pilot production of limestone calcined clay cement (LC 3) in India: the experience, Indian Concr. J. 90 (2016) 57–64.
[6] S. Bishnoi, S. Maity, M. Amit, S. Joseph, S. Krishnan, Pilot scale manufacture of limestone calcined clay cement: the Indian experience, Indian Concr. J. 88 (2014) 22–28.
[7] K.L. Scrivener, Options for the future of cements, Indian Concr. J. 88 (2014) 11–21.
[8] M. Antoni, J. Rossen, F. Martirena, K. Scrivener, Cement substitution by a combination of metakaolin and limestone, Cem. Concr. Res. 42 (2012) 1579–1589.
[9] R. Fernandez, F. Martirena, K.L. Scrivener, The origin of the pozzolanic activity of calcined clay minerals: a comparison between kaolinite, illite and montmorillonite, Cem. Concr. Res. 41 (2011) 113–122, https://doi.org/10.1016/j.cemconres.2010.09.013.
[10] V.L. Bonavetti, V.F. Rahhal, E.F. Irassar, Studies on the carboaluminate formation in limestone filler-blended cements, Cem. Concr. Res. 31 (2001) 853–859, https://doi.org/10.1016/S0008-8846(01)00491-4.
[11] G. Puerta-Falla, M. Balonis, G. Le Saout, G. Falzone, C. Zhang, N. Neithalath, G. Sant, Elucidating the role of the aluminous source on limestone reactivity in

cementitious materials, J. Am. Ceram. Soc. 98 (2015) 4076–4089, https://doi.org/10.1111/jace.13806.
[12] F. Avet, R. Snellings, A. Alujas, K. Scrivener, Development of a new rapid, relevant and reliable (R 3) testing method to evaluate the pozzolanic activity of calcined clays, Cem. Concr. Res. 85 (2016) 1–11, https://doi.org/10.1016/j.cemconres.2016.02.015.
[13] A. Tironi, M.A. Trezza, A.N. Scian, E.F. Irassar, Assessment of pozzolanic activity of different calcined clays, Cem. Concr. Compos. 37 (2013) 319–327, https://doi.org/10.1016/j.cemconcomp.2013.01.002.
[14] P.D. Tennis, M.D.A. Thomas, W.J. Weiss, State-of-the-Art Report on Use of Limestone in Cements at Levels of up to 15%, Portland Cement Association, 20111–78.
[15] I. Mohammadi, W. South, General purpose cement with increased limestone content in Australia, ACI Mater. J. 113 (2016) 335–347, https://doi.org/10.14359/51688703.
[16] ASTM:C595/C595M-13, Standard Specification for Blended Hydraulic Cements, ASTM International, 20131–13, https://doi.org/10.1520/C0595.
[17] K. Githachuri, M.G. Alexander, Durability performance potential and strength of blended Portland limestone cement concrete, Cem. Concr. Compos. 39 (2013) 115–121, https://doi.org/10.1016/j.cemconcomp.2013.03.027.
[18] S. Palm, T. Proske, M. Rezvani, S. Hainer, C. Müller, C.-A. Graubner, Cements with a high limestone content – mechanical properties, durability and ecological characteristics of the concrete, Constr. Build. Mater. 119 (2016) 308–318, https://doi.org/10.1016/j.conbuildmat.2016.05.009.
[19] B. Sabir, S. Wild, J. Bai, Metakaolin and calcined clays as pozzolans for concrete: a review, Cem. Concr. Compos. 23 (2001) 441–454, https://doi.org/10.1016/S0958-9465(00)00092-5.
[20] H.S. Al-Alaily, A.A.A. Hassan, Time-dependence of chloride diffusion for concrete containing metakaolin, J. Build. Eng. 7 (2016) 159–169, https://doi.org/10.1016/j.jobe.2016.06.003.
[21] J.M. Khatib, R.M. Clay, Absorption characteristics of metakaolin concrete, Cem. Concr. Res. 34 (2004) 19–29, https://doi.org/10.1016/S0008-8846(03)00188-1.
[22] M.F. Carrasco, G. Menéndez, V. Bonavetti, E.F.F. Irassar, Strength optimization of 'tailor-made cement' with limestone filler and blast furnace slag, Cem. Concr. Res. 35 (2005) 1324–1331, https://doi.org/10.1016/j.cemconres.2004.09.023.
[23] K. Vance, M. Aguayo, T. Oey, G. Sant, N. Neithalath, Hydration and strength development in ternary portland cement blends containing limestone and fly ash or metakaolin, Cem. Concr. Compos. 39 (2013) 93–103, https://doi.org/10.1016/j.cemconcomp.2013.03.028.
[24] G. Menéndez, V. Bonavetti, E.F. Irassar, Strength development of ternary blended cement with limestone filler and blast-furnace slag, Cem. Concr. Compos. 25 (2003) 61–67, https://doi.org/10.1016/S0958-9465(01)00056-7.
[25] A. Arora, G. Sant, N. Neithalath, Ternary blends containing slag and interground/blended limestone: hydration, strength, and pore structure, Constr. Build. Mater. 102 (2016) 113–124, https://doi.org/10.1016/j.conbuildmat.2015.10.179.
[26] S. Adu-Amankwah, M. Zajac, C. Stabler, B. Lothenbach, L. Black, Influence of Limestone on the Hydration of Ternary Slag Cements Samuel, 100, 201796–109, https://doi.org/10.1016/j.cemconres.2009.11.001.
[27] K. De Weerdt, M. Ben Haha, G. Le Saout, K.O.O. Kjellsen, H. Justnes, B. Lothenbach, Hydration mechanisms of ternary Portland cements containing limestone powder and fly ash, Cem. Concr. Res. 41 (2011) 279–291, https://doi.org/10.1016/j.cemconres.2010.11.014.
[28] IS 12269, Ordinary Portland Cement, 53 Grade—Specification, Bureau of Indian Standards, 20131–17.
[29] IS 516-04, Methods of Tests for Strength of Concrete, 1959, Bureau of Indian Standards, 20041–23.
[30] ASTM C469, Standard Test Method for Static Modulus of Elasticity and Poisson's Ratio of Concrete in Compression, ASTM International, 20141–5, https://doi.org/10.1520/C0469.
[31] ASTM C157, Standard Test Method for Length Change of Hardened Hydraulic-cement Mortar and, Annual Book of ASTM Standards, 8, 20161–7, https://doi.org/10.1520/C0157.
[32] FM5-578, Florida Method of Test for Concrete Resistivity as an Electrical Indicator of its Permeability, 20044–7.
[33] Resipod, Proceq, http://www.proceq.com/fileadmin/documents/proceq/products/Concrete/Resipod/English/resipod_SF_E_2013.06.19_low.pdf. n.d..
[34] ASTM C1202, Standard Test Method for Electrical Indication of Concrete's Ability to Resist Chloride Ion Penetration, American Society for Testing and Materials, 20121–8.
[35] NT Build 492, Concrete, Mortar and Cement-based Repair Materials: Chloride Migration Coefficient From Non-Steady-State Migration Experiments, NordTest, 19991–8.
[36] M.G. Alexander, Y. Ballim, J.R. Mackechnie, Durability Index Testing Procedure Manual, University of Cape Town, CoMSIRU, 20091–29, (Ver 1.0).
[37] M.G. Alexander, J.R. Mackechnie, Y. Ballim, Concrete Durability Index Testing Manual (Research Monograph No. 4), Department of Civil Engineering, University of Cape Town, 19991–33.
[38] M. Alexander, Y. Ballim, M. Santhanam, Performance specifications for concrete using the durability index approach, Indian Concr. J. 79 (2005) 41–46.
[39] Y. Bu, R. Spragg, W.J. Weiss, Comparison of the pore volume in concrete as determined using ASTM C642 and vacuum saturation, Adv. Civ. Eng. Mater. 3 (2014)20130090https://doi.org/10.1520/ACEM20130090.
[40] E. Berodier, K. Scrivener, Evolution of pore structure in blended systems, Cem. Concr. Res. 73 (2015) 25–35, https://doi.org/10.1016/j.cemconres.2015.02.025.
[41] Bureau of Indian Standard(BIS), Plain and Reinforced Concrete - Code of Practice, IS 456(4th Rev.), 2000, (New Delhi, India. doi:624.1834).
[42] Fédération Internationale du Béton, CEB-FIP Model Code 2010, vol. 1, 2010.
[43] B. Bissonnette, P. Pierre, M. Pigeon, Influence of key parameters on drying shrinkage of cementitious materials, Cem. Concr. Res. 29 (1999) 1655–1662, https://doi.org/10.1016/S0008-8846(99)00156-8.
[44] ACI Committee 209, Report on Factors Affecting Shrinkage and Creep of Hardened Concrete, American Concrete Institute, 200512, (IR-05).
[45] G. Sant, P. Lura, J. Weiss, Measurement of volume change in cementitious materials at early ages: review of testing protocols and interpretation of results, Transp. Res. Rec. 1979 (2006) 21–29, https://doi.org/10.3141/1979-05.
[46] J.J. Brooks, M.A. Megat Johari, Effect of metakaolin on creep and shrinkage of concrete, Cem. Concr. Compos. 23 (2001) 495–502, https://doi.org/10.1016/S0958-9465(00)00095-0.
[47] E. Güneyisi, M. Gesoğlu, K. Mermerdaş, Improving strength, drying shrinkage, and pore structure of concrete using metakaolin, Mater. Struct. 41 (2007) 937–949, https://doi.org/10.1617/s11527-007-9296-z.
[48] J.T. Ding, Z. Li, Effects of metakaolin and silica fume on properties of concrete, ACI Mater. J. 99 (2002) 393–398.
[49] J. Camiletti, A.M. Soliman, M.L. Nehdi, Effects of nano- and micro-limestone addition on early-age properties of ultra-high-performance concrete, Mater. Struct. 46 (2013) 881–898, https://doi.org/10.1617/s11527-012-9940-0.
[50] R.K. Dhir, M.C. Limbachiya, M.J. McCarthy, A. Chaipanich, Evaluation of Portland limestone cements for use in concrete construction, Mater. Struct. 40 (2007) 459–473.
[51] M. Bederina, Z. Makhloufi, T. Bouziani, Effect of limestone fillers the physic-mechanical properties of limestone concrete, Phys. Procedia 21 (2011) 28–34, https://doi.org/10.1016/j.phpro.2011.10.005.
[52] C. Varhen, I. Dilonardo, R.C. de Oliveira Romano, R.G. Pileggi, A.D. de Figueiredo, Effect of the substitution of cement by limestone filler on the rheological behaviour and shrinkage of microconcretes, Constr. Build. Mater. 125 (2016) 375–386.
[53] R.T. Committee, RILEM draft recommendation: TC-242-MDC multi-decade creep and shrinkage of concrete: material model and structural analysis*, Mater. Struct. 48 (2015) 753–770, https://doi.org/10.1617/s11527-014-0485-2.
[54] ACI 209R-92, Prediction of Creep, Shrinkage and Temperature Effects in Concrete Structures, 1997https://doi.org/10.1201/9780203882955.ch168.
[55] Fédération Internationale du Béton, CEB-FIP Model Code, vol. 1, 2010https://doi.org/10.1002/9783433604090.
[56] S. Feliu, J.A. Gonzalez, C. Andrade, Electrochemical Methods for On-site Determinations of Corrosion Rates of Rebars, 1276, ASTM International. STP, 1996107–118.
[57] P. Ghosh, Q. Tran, Influence of parameters on surface resistivity of concrete, Cem. Concr. Compos. 62 (2015) 134–145, https://doi.org/10.1016/j.cemconcomp.2015.06.003.
[58] J. Tanesi, A. Ardani, Surface Resistivity Test Evaluation as an Indicator of the Chloride Permeability of Concrete, U.S. Department of Transportation Federal Highway Adminstration, 20121–6.
[59] B.S. Dhanya, M. Santhanam, Performance evaluation of rapid chloride permeability test in concretes with supplementary cementitious materials, Mater. Struct. 50 (2017)67https://doi.org/10.1617/s11527-016-0940-3.
[60] Y. Dhandapani, M. Santhanam, Assessment of pore structure evolution in the limestone calcined clay cementitious system and its implications for performance, Cem. Concr. Compos. 84 (2017) 36–47.
[61] ACI-222R-01, ACI 222R-01 Protection of Metals in Concrete Against Corrosion Reported by ACI Committee 222, ACI-222R-01, 1, 20101–41.
[62] Y. Dhandapani, K. Vignesh, T. Raja, M. Santhanam, Development of the microstructure in LC3 systems and its effect on concrete properties, in: F. Martirena, A. Favier, K. Scrivener (Eds.), Calcined Clays for Sustainable Concrete: Proceedings of the 2nd International Conference on Calcined Clays for Sustainable Concrete, Springer, Netherlands, Dordrecht, 2018, pp. 131–140, https://doi.org/10.1007/978-94-024-1207-9_21.
[63] D. Bjegović, M. Serdar, I.S. Oslaković, F. Jacobs, H. Beushausen, C. Andrade, A.V. Monteiro, P. Paulini, S. Nanukuttan, Test Methods for Concrete Durability Indicators, RILEM TC 230-PSC Performance-based Specifications and Control of Concrete Durability, State-of-the-Art Report, 2015.
[64] R.B. Polder, W.H.A. Peelen, Electrical resistivity testing for as-built concrete performance assessment of chloride penetration, In: RILEM International Workshop on Performance-based Specification and Control of Concrete Durability, 2014, pp. 151–157.
[65] J. Gudimettla, G. Crawford, Resistivity tests for concrete—recent field experience, ACI Mater. J. 113 (2016) 505–512, https://doi.org/10.14359/51688830.
[66] B.S. Dhanya, M. Santhanam, Use of combined durability parameters for different exposure conditions, In: RILEM International Workshop on Performance-based Specification and Control of Concrete Durability, 2014, pp. 101–108.
[67] B.G. Salvoldi, H. Beushausen, M.G. Alexander, Oxygen permeability of concrete and its relation to carbonation, Constr. Build. Mater. 85 (2015) 30–37, https://doi.org/10.1016/j.conbuildmat.2015.02.019.
[68] M.G. Alexander, J.R. Mackechnie, Y. Ballim, Guide to the Use of Durability Indexes for Achieving Durability in Concrete Structures, Research Monograph, 199936.
[69] BS EN 206, BSI Standards Publication Concrete—Specification, Performance, Production and Conformity, 30, British Standard, 2013.
[70] C. Famy, A.R. Brough, H.F.W. Taylor, The C-S-H gel of Portland cement mortars: part I. The interpretation of energy-dispersive X-ray microanalyses from scanning electron microscopy, with some observations on C-S-H, AFm and AFt phase compositions, Cem. Concr. Res. 33 (2003) 1389–1398, https://doi.org/10.1016/S0008-8846(03)00064-4.
[71] H.M. Jennings, Model for the microstructure of calcium silicate hydrate in cement paste, Cem. Concr. Res. 30 (2000) 101–116, https://doi.org/10.1016/S0008-8846(99)00209-4.
[72] H.M. Jennings, Refinements to colloid model of C-S-H in cement: CM-II, Cem. Concr. Res. 38 (2008) 275–289, https://doi.org/10.1016/j.cemconres.2007.10.006.
[73] P.D. Tennis, H.M. Jennings, Model for two types of calcium silicate hydrate in the microstructure of Portland cement pastes, Cem. Concr. Res. 30 (2000) 855–863, https://doi.org/10.1016/S0008-8846(00)00257-X.